Amino Acids (2013) 44:151–159
DOI 10.1007/s00726-011-1083-z

ORIGINAL ARTICLE

Transglutaminase 2 interaction with small heat shock proteins mediate cell survival upon excitotoxic stress

Daniela Caccamo · Salvatore Condello · Nadia Ferlazzo · Monica Currò · Martin Griffin · Riccardo Ientile

Received: 30 June 2011 / Accepted: 8 September 2011 / Published online: 21 September 2011

Abstract Transglutaminase 2 has been postulated to be involved in the pathogenesis of central nervous system neurodegenerative disorders. However, its role in neuronal cell death remains to be elucidated. Excitotoxicity is a common event underlying neurodegeneration. We aimed to evaluate the protein targets for transglutaminase 2 in cell response to NMDA-induced excitotoxic stress, using SH-SY5Y neuroblastoma cells which express high tranglutaminase 2 levels upon retinoic acid-driven differentiation toward neurons. NMDA-evoked calcium increase led to transglutaminase 2 activation that mediated cell survival, as at first suggested by the exacerbation of NMDA toxicity in the presence of R283, a synthetic competitive inhibitor of transglutaminase active site. Assays of R283-mediated transglutaminase inhibition showed the involvement of enzyme activity in NMDA-induced reduction in protein basal levels of pro-apoptotic caspase-3 and the stress protein Hsp20. However, this occurred in a way different from protein cross-linking, given that macromolecular assemblies were not observed in our experimental conditions for both proteins. Co-immunoprecipitation experiments provided evidence for the interaction, in basal conditions, between transglutaminase 2 and Hsp20, as well as between Hsp20 and Hsp27, a major anti-apoptotic protein promoting caspase-3 inactivation and degradation. NMDA treatment disrupted both these interactions that were restored upon transglutaminase 2 inhibition with R283. These results suggest that transglutaminase 2 might be protective against NMDA-evoked excitotoxic insult in neuronal-like SH-SY5Y cells in a way, independent from transamidation that likely involves its interaction with the complex Hsp20/Hsp27 playing a pro-survival role.

Keywords Transglutaminase 2 · Excitotoxicity · Neuronal-like SH-SY5Y cells · Small heat shock proteins · Transglutaminase inhibitor R283

D. Caccamo · S. Condello · N. Ferlazzo · M. Currò · R. Ientile (✉)
Department of Biochemical, Physiological and Nutritional Sciences, University of Messina, Via C. Valeria, Policlinico Universitario, 98125 Messina, Italy
e-mail: ientile@unime.it

M. Griffin
School of Life and Health Sciences, Aston University, Birmingham, UK

Introduction

Transglutaminase 2 (TG2) belongs to a family of enzymes which catalyze calcium-dependent protein modifications, such as intra- or inter-molecular protein cross-linking, with formation of covalent γ-glutamyl-ε-lysine (GGEL) isopeptide bonds (*cross-links*), as well as, alternatively, polyamine incorporation into cell proteins or deamidation of specific glutamine residues in the absence of suitable amine acceptors (Folk and Finlayson 1977).

Multiple biochemical activities, i.e. acting as G protein, adaptor protein and cell surface adhesion mediator, as well as disulphide isomerase and serine/threonine kinase, distinguish TG2 from other TGs (Park et al. 2010), and account for TG2 involvement in a wide variety of physiological processes encompassing regulation of cytoskeleton, differentiation, apoptosis, cell migration, and wound healing, as well as in cell response to different stressors (Griffin et al. 2002; Ientile et al. 2007).

Moreover, an important pathogenetic role for TG2 has also been demonstrated in neurodegenerative disorders (Jeitner et al. 2009). TG2 is abundantly expressed in human

brain, being present in the amygdala, corpus callosum, cerebellum and frontal cortex. Notably, postmortem analysis of human brains of individuals affected by Alzheimer's disease, Parkinson's disease, and Huntington's chorea, has shown the co-localization of TG-catalysed cross-links with protein aggregates of disease-specific proteins (Jeitner et al. 2009).

These findings suggest that TG2 activation might play a key role in the mechanisms of central nervous system (CNS) cell death, although its role in neurodegeneration remains to be elucidated.

A number of factors, including excitotoxicity, oxidative stress, mitochondrial dysfunction, inflammation, and apoptosis, have been implicated in the massive cell loss observed in neurodegenerative diseases (Jellinger 2009). Interestingly, it has been demonstrated that TG2 expression and enzyme activity are dramatically increased in cell response to perturbations of calcium and redox state homeostasis induced by excitatory amino acids in primary cultures of neurons as well as astrocytes (Ientile et al. 2002; Caccamo et al. 2004; Jeitner et al. 2009).

In the light of these observations, the present work was aimed to evaluate the protein targets of TG activity in cell response to NMDA-induced excitotoxic stress.

To this purpose, we used the continuously dividing human neuroblastoma SH-SY5Y cells that have been largely employed to study neurodegenerative disorders. Indeed, SH-SY5Y cells may be easily induced to differentiate by retinoic acid (RA) into cells that are biochemically, ultrastructurally, and electrophysiologically similar to neurons, and are known to express high levels of TG2 upon *all*-trans RA-mediated cell differentiation (Tucholski et al. 2001).

Since retinoid response elements are present in the promoter of TG2, we chose to use RA as physiologically relevant ligand of the endogenous promoter rather than over-expressing the protein from an exogenous source, in order to physiologically increase the expression of TG2 protein while at the same time giving rise to a suitable differentiated cell model.

Materials and methods

Materials

Eagle's minimal essential medium (MEM), Ham's F12 medium, foetal bovine serum (FBS), and penicillin/streptomycin mixture were from Invitrogen Life Technologies (Milan, Italy). *All*-trans RA, NMDA, RIPA buffer, Fura2-AM, 3-(4, 5-methylthiazol-2-yl)-2, 5-diphenyl-tetrazolium bromide (MTT), Protein-G Agarose, anti-α-tubulin mouse monoclonal antibody (mAb), horseradish peroxidase-conjugated (HRP) anti-mouse secondary Ab, and other chemicals of analytical grade were from Sigma (Milan, Italy).

Mouse mAbs against caspase-3 and TG2 (CUB 7402) as well as anti-TG2 rabbit polyclonal Ab (clone Ab-4) were from NeoMarkers (BioOptica, Milan, Italy). Control mouse IgG as well as mouse mAb against Hsp27 were from Santa Cruz Biotechnology (DBA, Milan, Italy). Rabbit polyclonal Abs against Hsp20 and Hsp27 were from Upstate (Milllipore, Milan, Italy). HRP-conjugated anti-rabbit secondary Ab was from GE Healthcare (Milan, Italy), while streptavidin-HRP was from Pierce (CELBIO, Milan, Italy). Kodak X-ray film was from Kodak (Milan, Italy).

The cell permeable, active site-directed specific TG synthetic inhibitor R283, namely 1,3-dimethyl-2-[(2-oxo-propyl)thio]imidazolium chloride (Griffin M, Coutts IG, Saint R–Intl. Pub. Num.r WO 2004/1133603, GB patent PCT/GB2004/002569), as well as biotin-cadaverin were available from Prof. Martin Griffin.

Cell culture and differentiation

Human SH-SY5Y neuroblastoma cells were maintained in MEM/Ham's F12 (1:1) culture medium supplemented with 10% FBS, 2 mM L-glutamine, 10 U/ml penicillin, and 100 mg/ml streptomycin.

After three passages, cells were induced to differentiate by exposure to 10 μM RA in MEM/F12 (1:1) with 1% FBS for 5 days in vitro (DIV). Medium was renewed every 2 days.

SH-SY5Y cell differentiation toward a neuronal phenotype was assessed by microscopical examination, and Western blot analysis of α-tubulin expression.

NMDA treatment

Excitotoxic stress was triggered in 5 DIV RA-differentiated SH-SY5Y cells by 1 h exposure to NMDA (0.1–1 mM) in Locke's buffer, containing 2.3 mM $CaCl_2$, and lacking of Mg^{2+} in order to remove Mg^{2+} block of the NMDA receptor channels (Ientile et al. 2002).

After NMDA treatment, cells were washed, and re-incubated for 4–24 h in 1% FBS fresh culture medium devoid of RA.

Parallel inhibition experiments of TG activity were also carried out by incubating cell cultures with 1 mM NMDA in the presence/absence of the inhibitor R283, used at a dose of 250 μM that does not significantly affect cell viability, as previously reported (Beck et al. 2006). The TG inhibitor was added to the culture medium three hours before NMDA treatment.

Cell viability assay

To assess the effects of NMDA treatment on cell viability an MTT (3-(4,5-methylthiazol-2-yl)-2,5-diphenyl-tetrazolium bromide) reduction assay was performed. After treatment, differentiated SH-SY5Y cells, grown in 96-well culture plates, were incubated with fresh medium containing MTT (0.5 mg/ml) at 37°C for 4 and 24 h. Then, insoluble formazan crystals were dissolved in 100 µl of a 10% (*w/v*) SDS solution in HCl 0.01 M. The optical density in each well was evaluated by spectrophotometrical measurement at 540 nm with a Sunrise microplate reader (Tecan Italia, Cologno Monzese, Italy).

The percent cell viability was assessed by the absorbance ratio of treated versus untreated cells. All experiments were made in triplicate.

Determination of intracellular calcium concentration

The intracellular Ca^{2+} concentration ($[Ca^{2+}]_i$) in NMDA-treated and untreated SH-SY5Y cells was measured by using the cell membrane permeant fluorescent dye Fura2-AM. The cells were seeded in six-well plates at a density of 2.5×10^6/ml, and treated with NMDA as above described.

For Fura 2-AM loading, NMDA-treated and untreated cells were collected and incubated with the complete medium containing Fura 2-AM to a final concentration of 2 µM (stock solution: 1 mM in DMSO) for 45 min at 37°C. Then, cells were washed three times with HEPES buffer by centrifuging at 400×*g* for 2 min. Fluorescence was measured in 2 ml of cell suspension on a Perkin Elmer LS-3 fluorescence spectrophotometer, by dual excitation at 340 and 380 nm and emission at 510 nm. The ratio of fluorescence intensities excited by 340 or 380 nm was calculated after subtraction of the background fluorescence, i.e. cell auto-fluorescence.

The F340/F380 ratio was measured to estimate the internal Ca^{2+} concentration. The $[Ca^{2+}]_i$ was calculated using the equation: $[Ca^{2+}]_i = K_d\,[(R - R_{min})/(R - R_{max})] \times Sf2/Sf1$, where K_d is dissociation constant of Fura2-AM for (Ca^{2+}), R is ratio of fluorescence for Fura 2-AM at the two excitation wavelengths, i.e. F340/F380, measured without the addition of Triton X-100 or EGTA, R_{max} is ratio of fluorescence in the presence of calcium excess obtained by cell lysis with 0.1% Triton X-100, R_{min} is ratio of fluorescence in the presence of minimal calcium obtained by lysing the cells and then chelating all the Ca^{2+} with 0.5 M EGTA, Sf2 is the fluorescence of Ca^{2+} free form of Fura 2-AM at 380 nm excitation wavelength, and Sf1 is the fluorescence of Ca^{2+} bound form of Fura 2-AM at 380 nm excitation wavelength.

In situ TG activity assay

In situ TG activity was evaluated spectrophotometrically according to the method reported by Zhang et al. (1998), with a major modification being the use of biotin-cadaverin (BC) instead of 5-(biotinamido)pentylamine. TG activity in situ was calculated as a percentage of basal activity.

To visualize the protein substrates into which the BC had been incorporated, 7.5 µg of cell proteins were resolved on a 10% polyacrylamide SDS gel and transferred to nitrocellulose. Membrane blocking and incubation with HRP-conjugated streptavidin were carried out as reported by Zhang et al. (1998).

Western blotting

After treatment, SH-SY5Y cells were homogenized on ice. Proteins (30 µg) were separated by SDS-PAGE onto 10% gel, and transferred to nitrocellulose membranes. After blocking, membranes were incubated overnight at 4°C, on a rotating device, with mouse mAbs against different proteins (TG2, α-tubulin, caspase-3) (diluted 1:1,000–1:2,000 in 5% non-fat dry milk in TBS-T), and rabbit polyclonal Abs against either Hsp20 or Hsp27 (diluted 1:2,000 in 5% non-fat dry milk in TBS-T). After four times washing by TBS-T, blotted membranes were incubated for 2 h with HRP-conjugated anti-mouse (1:2,500 in 5% non-fat dry milk in TBS-T) or anti-rabbit (1:10,000 in 5% non-fat dry milk in TBS-T) secondary Abs, and developed by ECL chemiluminescence detection system kit using Kodak film. Bands were scanned and quantified by densitometric analysis with an AlphaImager 1200 System (Alpha Innotech, San Leandro, CA, USA), after normalisation against α-tubulin.

Immunoprecipitation assays

To perform co-immunoprecipitation assays, a new set of experiments was carried out in which untreated and treated RA-differentiated SH-SY5Y cells were collected 16 h after NMDA treatment, in order to anticipate either TG2 or Hsp20 protein degradation. Cells, harvested with PBS, were collected by centrifugation at 800×*g* for 10 min, and lysed by 20 min on ice incubation with RIPA buffer. Then, cell lysates (1 ml) were pre-cleared by incubation at 4°C for 30 min with control mouse IgG (0.25 µg), followed by addition of suspended Protein G-Agarose (20 µl; 25% *v/v*). IgG-Protein G agarose conjugates were pelleted by centrifugation at 1,000×*g* for 2 min at 4°C. Supernatants were collected and transferred to new microcentrifuge tubes. After protein quantification by Bradford assay, cell proteins (100 µg) were subjected to immunoprecipitation with 0.2 µg mouse mAb against either TG2 (CUB 7402) or

Hsp27. After 2 h of incubation at 4°C with the primary antibody, cell lysates were incubated overnight at 4°C with 20 µl of suspended Protein-G Agarose on a rotating device. Pellets were collected by centrifugation at 1,000×*g* for 2 min at 4°C, washed four times with RIPA buffer, and finally resuspended in 40 µl of 2× electrophoresis sample buffer. After boiling for 5 min, samples (20 µl) were subjected to SDS-PAGE on a 10% polyacrylamide gel, and electroblotting on nitrocellulose membranes; then, membranes were probed with rabbit polyclonal Ab against either TG2 (clone Ab-4), to confirm TG2 immunoprecipitation, or Hsp20 (diluted 1:2,500 in 5% non-fat dry milk in TBS-T). After extensive washing (4 times) with TBS-T, immunoblots were incubated with HRP-conjugated anti-rabbit Ab (diluted 1:5,000 in TBS-T). Immunoblots were developed by advanced ECL system.

Statistical analysis

All values are presented as mean ± SEM. Statistical analysis was performed using one-way ANOVA, followed by Newman–Keuls post-hoc test.

Results

After exposure to 10 µM RA for 5 DIV, SH-SY5Y neuroblastoma cells ceased proliferating, and differentiated with extending neuritic processes (not shown).

Differentiated SH-SY5Y cells were challenged for 1 h with NMDA (0.1–1 mM) in Locke's buffer, and then re-incubated up to 24 h in fresh culture medium devoid of RA to exclude RA effects on gene expression, in order to compare early (4 h) and delayed (24 h) effects of NMDA treatment.

A nearly fivefold increase of cytosolic Ca^{2+} concentration was observed in cell cultures treated for 1 h with 1 mM NMDA compared with untreated ones (477.8 ± 28.4 vs. 102.4 ± 8.3 nm; $p < 0.05$), while the exposure for the same time to 0.1 mM NMDA did not produce a significant calcium elevation (202.9 ± 14.7 vs. 152.4 ± 8.3 nm).

We next investigated whether NMDA-induced alterations of intracellular Ca^{2+} homeostasis were associated with cell death, given the reported toxicity of cytosolic Ca^{2+} increases when the Ca^{2+} concentration reaches a set-point between 0.3 and 1 µM (Arundine and Tymianski 2003).

Microscopical examination (not shown) as well as MTT reduction showed that the exposure to NMDA, even at the highest dose, did not significantly affect cell viability at early (4 h) after treatment or late (24 h) after treatment (Table 1).

Table 1 Effects of NMDA treatment on cell viability in RA-differentiated neuronal-like SH-SY5Y cells

	Viable cells (%)	
	4 h	24 h
Control	98.7 ± 0.8	97.3 ± 0.7
NMDA (0.1 mM)	96.3 ± 0.9	94.2 ± 0.8
NMDA (1 mM)	93.2 ± 0.7	85.7 ± 1.4
Control + R283 (250 µM)	92.3 ± 0.7	89.7 ± 0.4
NMDA (1 mM) + R283 (250 µM)	75.7 ± 1.5*	60.8 ± 1.6*

Cell viability was assessed as percentage of MTT reduction in comparison with control cells

* $p < 0.05$ in comparison to control cells. Data shown are mean ± SEM from five replicates

In the light of these results, all subsequent experiments were carried out using 1 mM NMDA, in order to achieve a relatively high Ca^{2+} level needed for TG2 activation.

RA-differentiated SH-SY5Y cells expressed high TG2 levels in basal conditions (Fig. 1a). However, in resting conditions, when the intracellular calcium concentration was around 100 nM, the enzyme remained inactive in the cytosol, as suggested by undetectable TG-catalyzed incorporation of BC into cell proteins as a measure of in situ activity.

Cell exposure to 1 mM NMDA early (4 h) produced a moderate increase in TG2 levels compared with controls (Fig. 1a), and a nearly fourfold increased in situ TG-mediated BC incorporation into cell proteins (Fig. 1b). NMDA-induced BC incorporation was strongly reduced (52%) by the pre-incubation with R283 (250 µM), the specific site-directed inhibitor of TG activity (Fig. 1b). The gel visualization of BC-labelled substrates showed the appearance of three novel substrates, ranging from 25 to 50 kDa, in NMDA-treated cells compared with control cells, that was almost suppressed in the presence of R283 (Fig. 1c).

Interestingly, the R283-mediated inhibition of TG2 activity exacerbated NMDA cytotoxicity, while, in parallel, did not significantly affect cell viability in control cells (Table 1).

Notably, a dramatic TG2 down-regulation was observed in control cell cultures at 24 h upon cell re-incubation in medium devoid of RA, while high TG2 protein levels, together with residual in situ enzyme activity, were found at the same time in NMDA-treated cells (Fig. 1a, b).

This suggested that molecular effects of NMDA treatment were able to counteract TG2 decrease following RA removal.

To assess whether in our experimental conditions high levels of TG2 would affect sensitivity of neuronal-like SH-SY5Y cells to NMDA-induced excitotoxicity, we investigated the expression and activation of caspase-3, the major executioner of apoptosis in neuronal cells.

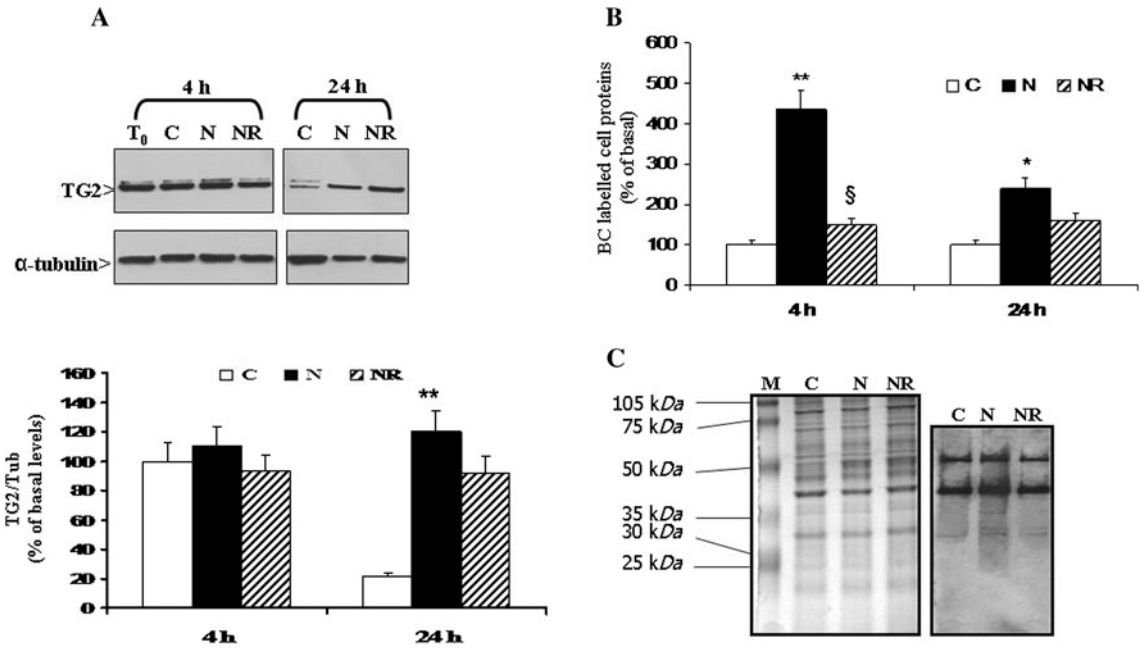

Fig. 1 NMDA treatment stimulates TG2 up-regulation and activation in RA-differentiated neuronal-like SH-SY5Y cells. **a**, **b** RA-differentiated neuronal-like SH-SY5Y cells were exposed for 1 h to 1 mM NMDA in the presence or absence of 250 μM R283, the inhibitor of TG active site. Then, cells were re-incubated in culture medium devoid of RA up to 24 h, and the effects of NMDA treatment on TG2 expression and activity were assessed at early (4 h) and delayed (24 h) time points. **a** Immunoblots and densitometric analysis of TG2 expression. **b** TG activity was evaluated by spectrophotometric detection of 1 mM BC incorporation into cell proteins throughout 4 and 24 h of incubation. BC was added to cell cultures immediately after NMDA treatment. All data shown are representative of at least three experiments. Values were calculated as percent of basal levels (T_0), and are shown as mean ± SEM. **c** Gel visualization of TG-catalyzed incorporation of BC into proteins as a measure of in situ activity: *left* Blue Coomassie staining of 10% SDS polyacrylamide gel, *right* representative blot of BC-labelled proteins. T_0 SH-SY5Y cells before NMDA treatment, *C* control cells, *N* NMDA-treated cells, *NR* NMDA-treated cells loaded with R283. *M* molecular weight protein marker. $^{*}p < 0.05$, and $^{**}p < 0.01$ significant differences in comparison with untreated cells; $^{\S}p < 0.01$, significant differences in comparison with NMDA-treated cells

Neuronal-like SH-SY5Y cells possessed a high basal content of pro-caspase-3. Neither increases in protein levels nor pro-caspase-3 processing into the active p17 subunit were observed at 4 h in NMDA-treated cells compared with untreated ones (Fig. 2). Instead, a strong caspase-3 down-regulation, that was reversed upon TG2 inhibition with R283, occurred 24 h after NMDA treatment in NMDA-exposed cells compared with control ones (Fig. 2).

Although we did not detect higher molecular weight species of pro-caspase-3, the results achieved in the presence of the TG2 inhibitor R283, i.e. the R283-mediated prevention of caspase-3 down-regulation, suggested the involvement of TG activity in the decrease of caspase-3 levels.

Therefore, we reasoned that inhibition of caspase-3 activation and caspase-3 decreases might be ascribed to a different TG2 enzyme function or even interaction of TG2 with other proteins playing an anti-apoptotic function.

We next examined the expression of cell stress proteins, such as heat shock proteins (HSPs) playing anti-apoptotic functions, focusing our investigations on small HSPs, i.e. Hsp27 and Hsp20, that have been shown to act as in vitro substrates for TG2 (Boros et al. 2004).

Western blot and immunoblot densitometric analysis showed that RA-differentiated SH-SY5Y cells contained high basal levels of Hsp27, as well as, at a lower extent, Hsp20 (Fig. 3).

The basal expression of both proteins was not significantly affected early (4 h) after NMDA treatment (Fig. 3). Instead, a dramatic reduction of Hsp20 levels, that became almost undetectable, was observed at 24 h in NMDA-treated cells compared with untreated ones (Fig. 3).

The pre-incubation with the TG2 inhibitor R283 did not significantly affect HSP expression at the early time of 4 h compared with NMDA-treated cells; in contrast, at 24 h after NMDA treatment the R283-mediated TG2 inhibition was accompanied by the reversal of the NMDA-induced Hsp20 down-regulation.

These data indicated that NMDA-induced TG2 activation was directly involved in the late decrease of cytosolic levels of Hsp20.

To verify whether TG2 physically interacted with Hsp20 in our cell paradigm of NMDA-induced excitotoxicity, we performed co-immunoprecipitation experiments that were carried out 16 h after NMDA treatment in order to

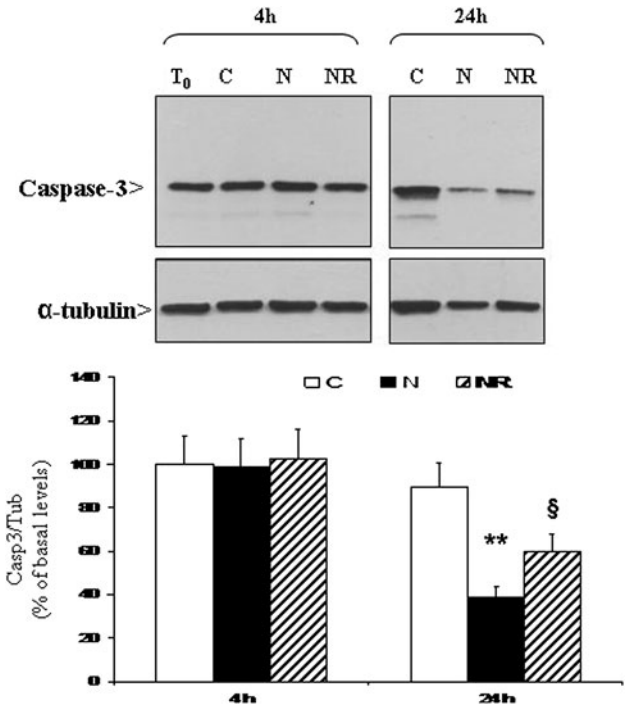

Fig. 2 NMDA-increased TG activity is involved in caspase-3 down-regulation in neuronal-like SH-SY5Y cells. Western blot and immunoblot densitometric analysis of caspase-3 expression. T_0 RA-differentiated SH-SY5Y cells before NMDA treatment, *C* control cells, *N* NMDA-treated cells, *NR* NMDA-treated cells loaded with R283. All data are representative of at least three experiments. Values were calculated as percent of basal levels (T_0), and are shown as mean ± SEM. $^{**}p < 0.01$, significant differences in comparison with untreated control cells; $^{\S}p < 0.05$, significant differences in comparison with NMDA-treated cells

anticipate the NMDA-induced down-regulation of Hsp20 as well as the strong decrease of TG2 protein levels in the controls.

Interestingly, TG2 and Hsp20 were co-immunoprecipitated both in NMDA-treated cells and untreated ones. The intensity of Hsp20 immunoreactive band was strongly reduced in NMDA-treated cells, likely due to Hsp20 degradation. Notably, the pre-incubation with R283 restored Hsp20 control levels (Fig. 4).

This suggested that TG2 interacted with Hsp20 in basal conditions, and that NMDA-induced TG2 activation led to Hsp20 degradation.

Taken together, these data indicate that TG2 constitutively interacts with Hsp20 in RA-differentiated SH-SY5Y cells, and that this interaction was disrupted when cells were exposed to NMDA. However, the specific inhibition of NMDA-induced TG2 activation by R283 reversed such effects.

Given the reported association of Hsp20 with Hsp27 in different tissues (Boros et al. 2004), we wondered whether Hsp20, in turn, interacted with Hsp27 in our cell stress paradigm.

New co-immunoprecipitation experiments using a mouse monoclonal antibody against Hsp27, followed by immunoblotting for Hsp20, resulted in a detectable interaction between these two proteins in untreated cells (Fig. 4), indicating a constitutive Hsp27/Hsp20 heteromeric association in RA-differentiated SH-SY5Y cells.

The interaction between Hsp20 and Hsp27 was disrupted upon NMDA treatment and was restored upon TG2 inhibition by R283 (Fig. 4).

Discussion

Overexpressed TG2 has been reported to either exert pro- or anti-apoptotic effects in cultured cells depending upon the type of cell, the kind of stressor, its activity levels and subcellular localization (Fèsus and Szondy 2005).

Here, we show that high TG2 levels, associated with RA-induced differentiation of neuroblastoma SH-SY5Y cells towards neuronal phenotype, resulted in cell survival against excitotoxic stress evoked by the exposure to high NMDA doses (1 mM).

Excitotoxicity, triggered by neuronal cell stimulation with excitatory aminoacids leading to disturbances of the intracellular calcium homeostasis, is thought to be a major mechanism contributing to neuronal loss during CNS ischemia, trauma, and neurological disorders (Jellinger 2009).

In our cell paradigm of excitotoxicity, despite a nearly fivefold increase of cytosolic calcium concentration NMDA treatment did not early induce a significant cell loss, neither did it delay the appearance of apoptotic features, as demonstrated by failure of the activation of caspase-3, the major apoptosis executioner in neurons.

Notably, the rise in Ca^{2+} intracellular levels triggered TG activation that was found to be involved in SH-SY5Y cell survival, as at first suggested by the exacerbation of NMDA toxicity upon specific inhibition of TG2 active site with R283.

These results are in contrast with our previous in vitro observations showing that NMDA treatment—at lower doses (100 μM) than those used in the present work—increased TG2 expression and activity which were associated with apoptotic features in primary cerebellar granule cells (Ientile et al. 2002; Caccamo et al. 2004).

Moreover, the use of TG2 transgenic mice has provided evidence that TG2 over-expression in the CNS potentiates excitotoxicity-induced neuronal cell damage (Tucholski et al. 2006). However, neither the identification of TG activity downstream targets, that play a role in the excitotoxic cell death process, nor the elucidation of the mechanisms by which over-expressed TG2 facilitates neuronal death, have ever been addressed in in vivo or in vitro models of excitotoxic insult.

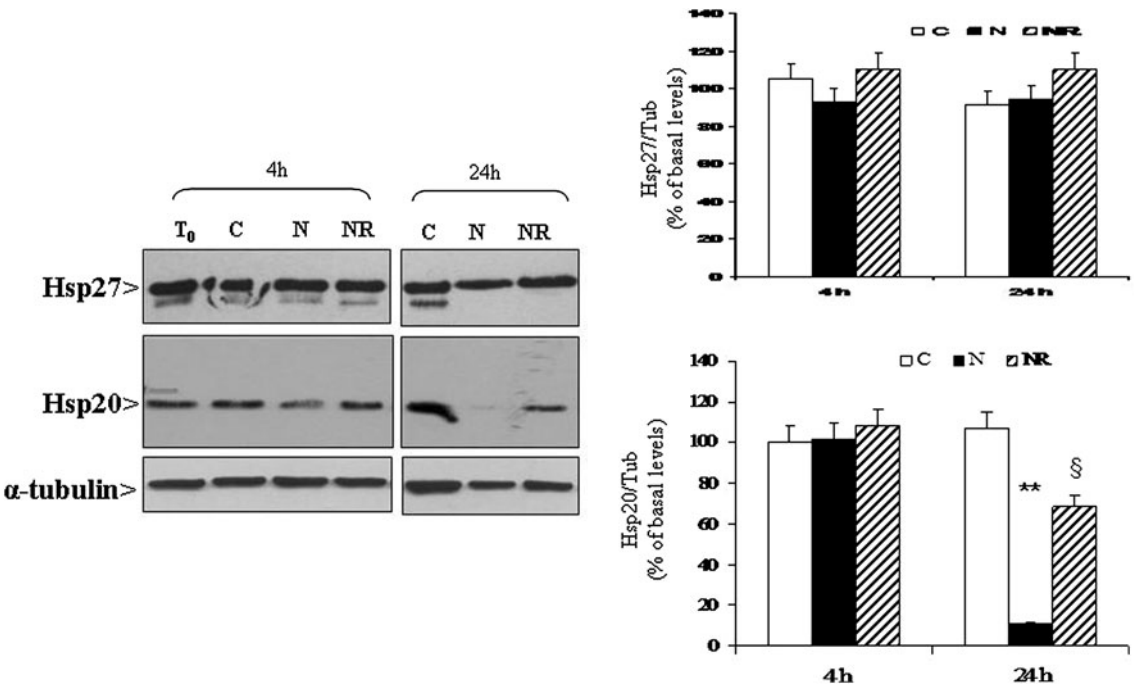

Fig. 3 NMDA-induced TG2 activation is involved in the reduction of Hsp20 levels in neuronal-like SH-SY5Y cells. Western blot analysis (*left*) and densitometric analysis (*right*) of the expression of cell stress proteins, such as the inducible Hsp27 and Hsp20, in untreated cells (*C*) and NMDA-treated ones in the absence (*N*) or presence of R283 (*NR*), compared with RA-differentiated SH-SY5Y cells before NMDA treatment (T_0). All data are representative of at least three experiments. Values were calculated as percent of basal levels (T_0), and are shown as mean ± SEM. $^{**}p < 0.01$, significant differences in comparison with untreated control cells; $^{\S}p < 0.01$, significant differences in comparison with NMDA-treated cells

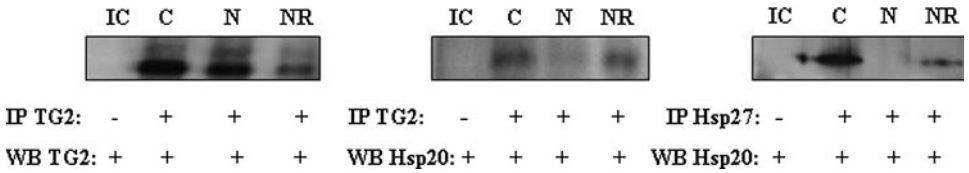

Fig. 4 NMDA-induced TG2 activation disrupts the constitutive interaction of TG2 with Hsp20 and leads to Hsp20 degradation in neuronal-like SH-SY5Y cells. Co-immunoprecipitation experiments showed the interaction between TG2 and Hsp20, and also between Hsp20 and Hsp27. Results shown are representative of three separate experiments. *IC* immunoprecipitation control in which the immunoprecipitating antibody was omitted, *C* control cells, *N* NMDA-treated cells, *NR* NMDA-treated cells loaded with R283

We wondered about the role of TG2 in molecular pathways underlying SH-SY5Y cell resistance to NMDA-induced excitotoxic stress.

Previous observations, in a different experimental model of neurotoxicity, have shown that the inhibition of over-expressed TG2 in SH-SY5Y cells reversed the amelioration of apoptotic response (Beck et al. 2006). In this regard, it is worthy to note that overexpressed TG2 has been reported to be protective against apoptosis when its crosslinking activity is dormant (Fèsus and Szondy 2005; Gundemir and Johnson 2009).

Given that TG2 cross-linking occurs at a threshold Ca^{2+} concentration of about 1 mM (Smethurst and Griffin 1996), it is reasonable to hypothesize that, in our experimental conditions, NMDA-increased cytosolic Ca^{2+} levels might mediate other TG2 enzyme functions, different from cross-linking, playing a protective role against excitotoxicity.

Moreover, it should be remarked that the extent of NMDA-induced TG activation was assessed, as current practice for TG activity assays, by measuring the incorporation of BC, an exogenously added polyamine, into cell proteins. By this way, we were able to provide evidence that the NMDA-evoked Ca^{2+} rise activated the TG-mediated in situ polyamination that may take place at intracellular Ca^{2+} levels lower than 1 mM. Notably, the gel visualization of BC labelled cell proteins showed the appearance of at least three novel TG2 substrates for TG enzyme activity, with molecular weight ranging between around 25 and 50 kDa, in NMDA-treated cells compared with controls.

Our preliminary data indicate that the NMDA-induced TG activation in neuronal-like SH-SY5Y cells was involved in the reduction in cytosolic levels of pro-apoptotic caspase-3 and the stress protein Hsp20. Indeed, caspase-3 has been reported to be a substrate for TG2 cross-linking activity in cell apoptosis (Yamaguchi and Wang 2006), and Hsp20 was shown to be in vitro crosslinked by TG2 (Boros et al. 2004). However, in our experimental conditions we did not detect macromolecular assemblies for both proteins. Whether or not these proteins may act as direct substrates for TG-catalysed polyamination has to be further investigated, even if this seems not likely for Hsp20, having a molecular weight lower than that observed for putative TG activity substrates upon SDS gel electrophoresis.

Here, we show, by the help of co-immunoprecipitation experiments, that TG2 interacts with Hsp20, and that this interaction is disrupted upon NMDA-induced TG2 activation, which results in Hsp20 degradation.

Interestingly, Hsp20, a chaperone-like protein initially identified as a by-product of the purification of Hsp27, has been reported to occur together with Hsp27 as heteromeric and dynamic complexes, that are modulated by both phosphorylation and/or macromolecular association with specific proteins, and usually dissociate from the aggregated form in response to cell stress (Boros et al. 2004).

Notably, Hsp27 has been shown to favour the proteasomal degradation of certain proteins under stress conditions and is generally considered an essential inhibitor of the proteolytic processing and activation of the apoptosis initiator pro-caspase-3 (Stetler et al. 2009). Indeed, neuronal-like SH-SY5Y cells possessed high basal levels of procaspase-3 that underwent NMDA-induced degradation, partly prevented by the specific inhibition of TG2 with R283.

The present observations raise the possibility that TG2 interaction with Hsp20 upon NMDA treatment might modulate the anti-apoptotic functions of the complex Hsp27/Hsp20, including, among others, the suppression of caspase-3 activation and the promotion of caspase-3 proteasomal degradation. This modulatory effect could take place without necessarily involving TG2 enzyme activity, since TG2 has already been shown to be protective against cell death in a way, independent from transamidation, that likely involves its physical association with other proteins playing a pro-survival or apoptotic role (Filiano et al. 2008; Gundemir and Johnson 2009). Notably, Hsp27 has also been identified as a "scaffold" protein, leading to the activation of pro-survival signalling molecules, such as MAPK-activated protein kinase-2 and the serine/threonine kinase Akt, which results in cytoprotection in different model of neuronal injury (Stetler et al. 2009).

Given that Hsp27 has been reported to be among the most potent suppressors of neurodegeneration induced by accumulation of toxic protein aggregates (Stetler et al. 2009), TG2 interaction with small HSP complexes could assume a relevant biological role and is worthy to be more extensively characterized.

Acknowledgments This work was partly funded by Aston University.

Conflict of interest There is no conflict of interest.

References

Arundine M, Tymianski M (2003) Molecular mechanisms of calcium-dependent neurodegeneration in excitotoxicity. Cell Calcium 34:325–337

Beck KA, De Girolamo LA, Griffin M, Billett EE (2006) The role of tissue transglutaminase in 1-methyl-4-phenylpyridinium (MPP+)-induced toxicity in differentiated human SH-SY5Y neuroblastoma cells. Neurosci Lett 405:46–51

Boros S, Kamps B, Wunderink L, de Bruijn W, de Jong WW, Boelens WC (2004) Transglutaminase catalyzes differential crosslinking of small heat shock proteins and amyloid-beta. FEBS Lett 576(1–2):57–62

Caccamo D, Currò M, Cusumano G, Crisafulli G, Ientile R (2004) Excitotoxin-induced changes in tranglutaminase during differentiation of cerebellar granule cells. Amino Acids 26:197–201

Fèsus L, Szondy Z (2005) Transglutaminase 2 in the balance of cell death and survival. FEBS Lett 579:3927–3302

Filiano AJ, Bailey CD, Tucholski J, Gundemir S, Johnson GV (2008) Transglutaminase 2 protects against ischemic insult, interacts with HIF1beta, and attenuates HIF1 signaling. FASEB J 22(8):2662–2675

Folk JE, Finlayson JS (1977) The epsilon-(gamma-glutamyl)lysine crosslink and the catalytic role of transglutaminases. Adv Protein Chem 31:1–133

Griffin M, Casadio R, Bergamini CM (2002) Transglutaminases: nature's biological glues. Biochem J 368(Pt 2):377–396

Gundemir S, Johnson GV (2009) Intracellular localization and conformational state of transglutaminase 2: implications for cell death. PLoS One 4(7):e6123

Ientile R, Caccamo D, Macaione V, Torre V, Macaione S (2002) NMDA-evoked excitotoxicity increases tissue transglutaminase in cerebellar granule cells. Neuroscience 115(3):723–729

Ientile R, Caccamo D, Griffin M (2007) Tissue transglutaminase and the stress response. Amino Acids 33:385–394

Jeitner TM, Pinto JT, Krasnikov BF, Horswill M, Cooper AJL (2009) Transglutaminases and neurodegeneration. J Neurochem 109: 160–166

Jellinger KA (2009) Recent advances in our understanding of neurodegeneration. J Neural Transm 116(9):1111–1162

Park D, Choi SS, Ha KS (2010) Transglutaminase 2: a multi-functional protein in multiple subcellular compartments. Amino Acids 39:619–631

Smethurst PA, Griffin M (1996) Measurement of tissue transglutaminase activity in a permeabilized cell system: its regulation by Ca^{2+} and nucleotides. Biochem J 313:803–808

Stetler RA, Signore AP, Gao Y, Cao G, Chen J (2009) HSP27: mechanisms of cellular protection against neuronal injury. Curr Mol Med 9(7):863–872

Tucholski J, Lesort M, Johnson GVW (2001) Tissue transglutaminase is essential for neurite outgrowth in human neuroblastoma SH-SY5Y cells. Neuroscience 102(2):481–491

Tucholski J, Roth KA, Johnson GVW (2006) Tissue transglutaminase overexpression in the brain potentiated calcium-induced hippocampal damage. J Neurochem 97:582–594

Yamaguchi H, Wang HG (2006) Tissue transglutaminase serves as an inhibitor of apoptosis by cross-linking caspase 3 in thapsigargin-treated cells. Mol Cell Biol 26(2):569–579

Zhang J, Lesort M, Guttmann RP, Johnson GVW (1998) Modulation of the in situ activity of tissue transglutaminase by calcium and GTP. J Biol Chem 273:2288–2295